# PRELIMINARY RESULTS ON CP-VIOLATING PHENOMENA IN THE KTEV EXPERIMENT AT FERMILAB

Richard Kessler
Enrico Fermi Institute
University of Chicago
Chicago, Illinois 60637

ABSTRACT

These proceedings will discuss some preliminary results from the KTeV experiment at Fermilab, with an emphasis on CP violation in the kaon system. Direct CP-violating topics include the measurement of $\mathrm{Re}(\epsilon'/\epsilon)$ and searches for the decays $K_L \to \pi^0\nu\bar{\nu}$ and $K_L \to \pi^0 e^+ e^-$. A new indirect CP-violating observable in the decay $K_L \to \pi^+\pi^- e^+ e^-$ is also discussed.

# 1 Introduction

Since the early 1960s, there have been three observations of CP-violating phenomena in particle physics: $K_L \to 2\pi$, the rate asymmetry between $\Gamma(K_L \to \pi^+ e^- \nu)$ and $\Gamma(K_L \to \pi^- e^+ \nu)$ (and similarly for $K_L \to \pi\mu\nu$), and the interference between $K_{L,S} \to \pi^+\pi^-\gamma$. All of these CP-violating effects are in the kaon system and can be described by a tiny asymmetry in the $K^0 \leftrightarrow \overline{K^0}$ mixing, which is usually referred to as "indirect" CP violation (CPV). The interesting question that KTeV is designed to study is whether CPV can be seen "directly" in decay amplitudes. With at least three families of quarks and leptons, the Standard Model (SM) allows for direct CPV which can be conveniently parameterized by the CKM parameter $\eta$.

The KTeV experiment is searching for three effects that are expected to exhibit direct CPV and provide information on the value of the CP-violating parameter $\eta$. Most of our data taking was dedicated to collecting $K_{L,S} \to \pi^+\pi^-$ and $K_{L,S} \to \pi^0\pi^0$ decays to measure $\mathrm{Re}(\epsilon'/\epsilon)$. We have also searched for the decays $K_L \to \pi^0\nu\bar{\nu}$ and $K_L \to \pi^0 e^+ e^-$; the former is expected to be "purely" direct CP violating, i.e., the rate is proportional to $|\eta|^2$, while the latter is expected to have both CP-conserving (CPC) and CP-violating contributions. New data on the $K_L \to \pi^0\gamma\gamma$ decay are presented, which helps unravel the CPC contribution to $K_L \to \pi^0 e^+ e^-$. In addition to our direct CP-violating searches, we have also observed the decay $K_L \to \pi^+\pi^- e^+ e^-$ which is expected to have an indirect CP-violating asymmetry in the angle between the $\pi^+\pi^-$ and $e^+e^-$ decay planes.

# 2 The KTeV Detector

The kaon beams are produced by an 800 GeV primary proton beam that strikes a BeO target ($3 \times 3 \times 305$ mm$^3$). Roughly half of the $3 \times 10^{12}$ protons per spill interact in the target while the other half are absorbed in a beam dump. A large sweeping magnet downstream from the beam dump effectively sweeps muons from both the primary target and the dump so that the muon flux hitting the detector is less than 100 kHz. Two identical sets of collimators produce two secondary neutral beams at $\pm 0.8$ mrad in the horizontal view. A set of beryllium and lead absorbers, 20 meters from the target, reduced the fraction of neutrons and photons in the beam.

The two kaon beams that enter the fiducial volume are illustrated in Fig. 1, which shows the detector configuration used to measure $\mathrm{Re}(\epsilon'/\epsilon)$. The vacuum decay region is from about 120 to 159 meters from the primary target. Following the vacuum region, helium bags are used to fill the volumes between detector elements. The $K_L$ beam is realized by placing the detector sufficiently far from the primary target so that the $K_S$ component has decayed away; the $K_S$ beam is made by sending one of the $K_L$ beams into a fully active 1.7 meter long regenerator made of a plastic scintillator.

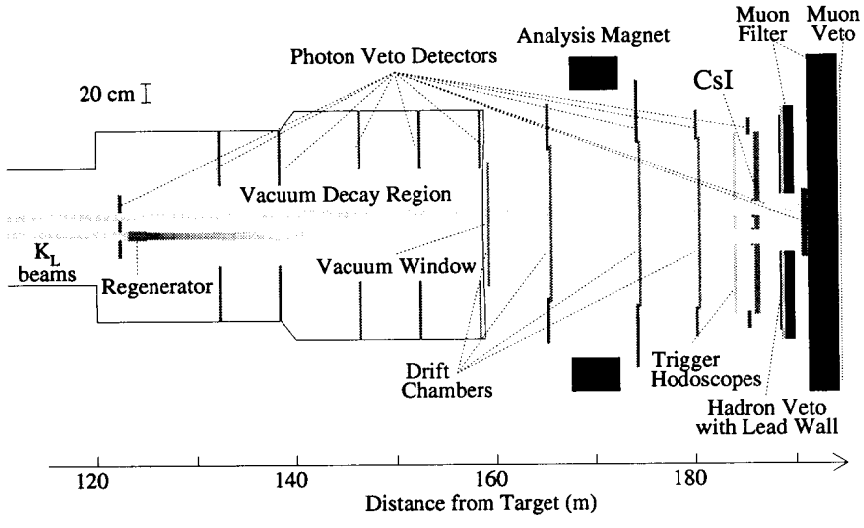


Fig. 1. The KTeV detector configuration used for the measurement of $\mathrm{Re}(\epsilon'/\epsilon)$.

The momenta of charged tracks are measured with four drift chambers, two on each side of an analysis magnet (0.4 GeV/c kick in X-view). A CsI electromagnetic calorimeter is used to measure the position and energy of photons and electrons. The inner $1.2 \times 1.2$ m$^2$ region consists of 2232 small crystals, each $0.025 \times 0.025 \times 0.500$ m$^3$; the outer region consists of 868 large crystals, each $0.050 \times 0.050 \times 0.500$ m$^3$. A nearly hermetic photon veto system is used to veto events in which one or more particles escape the detector. A set of trigger hodoscopes just upstream of the CsI calorimeter is used to trigger charged particles. Both the CsI calorimeter and the trigger hodoscopes

have two $0.15 \times 0.15$ m$^2$ holes to allow the high intensity neutral beams to pass through.

Rare kaon decay searches used the detector configuration shown in Fig. 1 with the following differences: (i) the regenerator and most upstream photon vetoes were removed to provide two identical $K_L$ beams and a longer decay region, (ii) a set of nine Transition Radiation Detectors (TRD) were installed downstream from the last drift chamber to provide additional separation between pions and electrons, (iii) the $K_L$ flux in the decay volume was several times higher, and (iv) the magnet kick was reduced from 0.4 GeV/c to 0.2 GeV/c in order to increase the acceptance for many-body decays.

# 3 Direct CP-Violating Searches

## 3.1 Re($\epsilon'/\epsilon$)

We do not yet have a result on the measurement of Re($\epsilon'/\epsilon$) so I will just make a few comments about our analysis and the critical systematic issues. We are aiming to extract a first result using about 25% of our total data set. The calibration and alignment has been completed for the CsI, drift chambers, and photon vetos. The statistics of this data set is shown in Table 1 and leads to a statistical uncertainty of $3 \times 10^{-4}$ on Re($\epsilon'/\epsilon$).

| $\epsilon'/\epsilon$ mode | Events | Bkg./signal |
|---|---|---|
| Vac ($K_L \to$) $\pi^0\pi^0$ | $1.0 \times 10^6$ | 0.8% |
| Reg ($K_S \to$) $\pi^0\pi^0$ | $1.6 \times 10^6$ | 1.5% |
| Vac ($K_L \to$) $\pi^+\pi^-$ | $1.9 \times 10^6$ | 0.1% |
| Reg ($K_S \to$) $\pi^+\pi^-$ | $3.9 \times 10^6$ | 0.1% |

Table 1. $K \to \pi\pi$ statistics under analysis for the first result on Re($\epsilon'/\epsilon$).

The most serious systematic issue is related to understanding the $K_{L,S} \to \pi^+\pi^-$ acceptance for tracks that hit the beam region of the drift chambers. The size of this region is $\sim 0.1 \times 0.1$ m$^2$ in each of the two beams, and about one-fourth of the $K_{L,S} \to \pi^+\pi^-$ events have at least one track that goes through this region of a drift chamber. A combination of high intensity and damage to the wires in the beam regions resulted in higher inefficiencies, and late hits in which the primary drift electrons did not fire the discriminator. These two effects cause tracks to be lost in the reconstruction and it adds tails to the distributions that we cut on the analysis. This results in a slight deficit of events in the beam region when compared to the Monte Carlo simulation, and is illustrated in Fig. 2; the beam region shows a percent level loss in the data that is not predicted by the Monte Carlo. This loss is not seen for events that lie outside the beam regions.

We are currently attempting to improve our simulation using detailed maps of the various chamber pathologies. With no understanding of the chamber performance we would have to assign a systematic uncertainty which is comparable to the statistical uncertainty; therefore, even a modest improvement in the simulation may help reduce the uncertainty for our first result.

The critical systematic issues for $K_{L,S} \to \pi^0\pi^0$ are related to the CsI calibration at low energies and the background. The CsI calibration below 4 GeV is not as well determined because the 0.4 GeV/c magnet kick swept away low-energy electrons from $K_L \to \pi e\nu$ decays that were used to calibrate the CsI response. About 25% of our $K_{L,S} \to \pi^0\pi^0$ events have at least one photon with an energy between 2 and 4 GeV. We are using $K_L \to \pi^+\pi^-\pi^0$ and $K_L \to 3\pi^0$ events to improve our understanding of low energy photons in the CsI.

The other neutral mode issue is related to the $K_{L,S} \to \pi^0\pi^0$ background, which is at the 1% level, and therefore, must be understood to within several percent of itself. To achieve this we have done detailed simulations of regenerator scatters, $K_L \to 3\pi^0$ decays with two undetected photons, collimator scatters, and hadronic $2\pi^0$ production off the edge of the regenerator. The largest background to $K_{L,S} \to \pi^0\pi^0$ is from kaons that scatter in the regenerator, but whose center of energy still lies within the coherent (i.e., $0^0$ scatter) beam profile. These small scatters cannot be identified in $2\pi^0$ decays, but they are easily detected in the charged $K^0 \to \pi^+\pi^-$ decays. The acceptance-corrected scatter distribution from the charged decays was parameterized as a function of its transverse momentum and decay time, and the result was fed into a Monte Carlo to simulate $2\pi^0$ decays from scattered kaons. This Monte Carlo background prediction for $2\pi^0$ decays is shown in Fig. 3 for the $Y$-view center of energy. The shape of the background distribution is based on the charged decays; the background scale comes from normalizing the data to the simulation for events in a region that has only background and no coherent signal (i.e., the side-bands in Fig. 3).

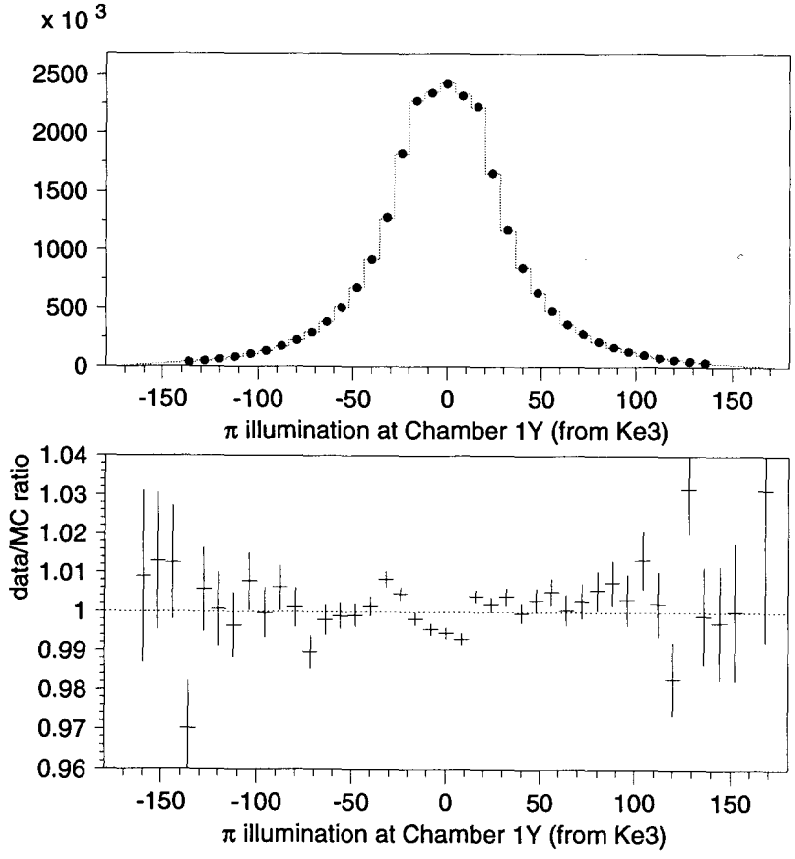


Fig. 2. The $Y$-view illumination at the first drift chamber is shown for pions from $K^0 \to \pi e\nu$. A cut requiring the beam region in the $X$-view has been applied. The dots are data, the histogram is Monte Carlo *without* detailed chamber simulations, and the ratio is shown in the lower plot. Each bin corresponds to half of a drift chamber cell (3.175 mm). The beam region occupies the central $\pm 16$ half-cells.

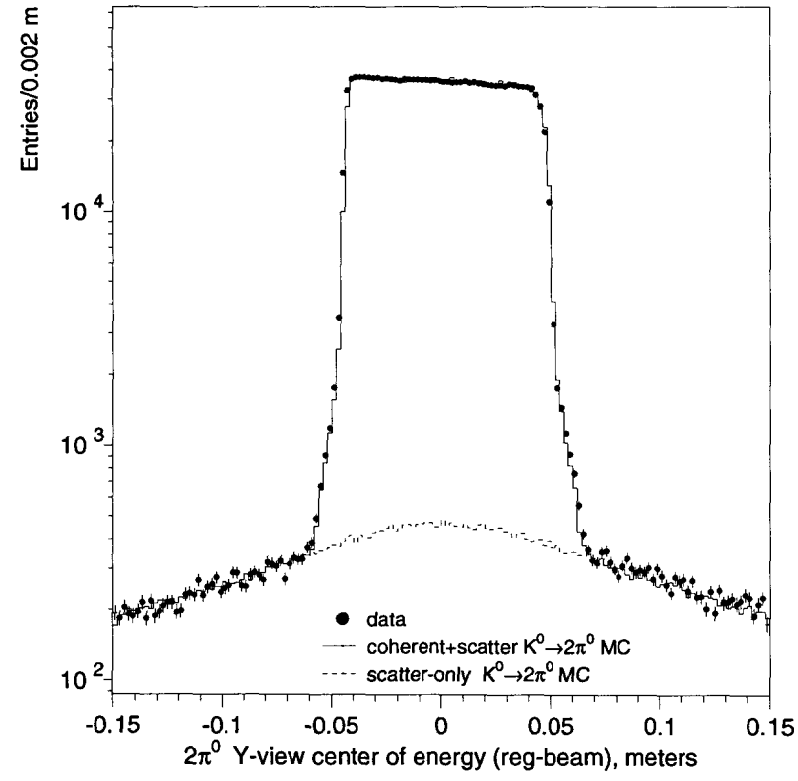


Fig. 3. *Preliminary* four-photon center of energy (meters) in the $Y$-view is shown for $2\pi^0$ decays in the regenerator beam. All other offline analysis cuts have been applied, including a cut on the $X$-view center of energy. The data are shown by the solid dots. The dashed histogram is from a background Monte Carlo simulation of kaon scatters in the regenerator. The histogram overlay is the Monte Carlo background (dashed) plus the coherent signal.

### 3.2 $K_L \to \pi^0\nu\bar{\nu}$

For the decay $K_L \to \pi^0\nu\bar{\nu}$, we have made two searches using different techniques. The first method used the decay $\pi^0 \to \gamma\gamma$ (Ref. 1), and the other method used the Dalitz decay $\pi^0 \to e^+e^-\gamma$ (Ref. 2). The advantage of the first method is that the branching ratio into two photons is 80 times larger and the acceptance is several times larger than for the Dalitz decay; the advantage of the second method is that the charged vertex information helps to reduce backgrounds. The $\pi^0 \to \gamma\gamma$ method resulted in one candidate which was consistent with the expected background, and gave a 90% confidence upper limit on the branching fraction of $1.6 \times 10^{-6}$. The $\pi^0 \to e^+e^-\gamma$ method resulted in no candidates and a 90% confidence upper limit of $5.9 \times 10^{-7}$. It should be noted that the $\pi^0 \to e^+e^-\gamma$ method required 50 times more data collection time and 50 times more $K_L$ flux than that used for the $\pi^0 \to \gamma\gamma$ method, yet it only improved the upper limit by a factor of three. This suggests that the path to reaching the SM prediction of $B_{SM}(K_L \to \pi^0\nu\bar{\nu}) \sim 3 \times 10^{-11}$ is via the $\pi^0 \to \gamma\gamma$ mode. The $\pi^0 \to \gamma\gamma$ technique was limited in our experiment by background due to hadronic $2\pi^0$ production off the vacuum window, in which two photons escaped detection and the other two photons reconstructed as a $\pi^0$ inside the decay volume.

I would like to finish this section with a few comments about future prospects for $K_L \to \pi^0\nu\bar{\nu}$ searches using the $\pi^0 \to \gamma\gamma$ decay. A dedicated $K_L \to \pi^0\nu\bar{\nu}$ experiment will have to remove as much material as possible between the decay volume and the detector to reduce the hadronic $2\pi^0$ background from neutron interactions. Another challenge for the $\pi^0 \to \gamma\gamma$ method will be to sufficiently suppress backgrounds from the dominant neutral decay modes $K_L \to 2\pi^0$ and $K_L \to 3\pi^0$, which will require efficient photon detection down to tens of MeV. The final and perhaps most challenging task is to make detectors that operate in a high rate environment with good signal efficiency. In particular, the photon veto system must be very efficient in detecting low-energy photons from background sources, yet at the same time, it should not reject too much signal due to accidental losses.

The difficulty in the photon veto system is well illustrated by our own analysis with two very different kaon fluxes. The $K_L \to \pi^0\nu\bar{\nu}$ search using $\pi^0 \to \gamma\gamma$ used just one kaon beam with reduced size ($0.04 \times 0.04$ m$^2$ at the CsI) to improve the transverse momentum measurement of the two detected photons. A beryllium absorber was placed far upstream to reduce the neutron/kaon ratio, and further reduced the kaon flux by a factor of three. The resulting kaon flux for this measurement was $\sim$ 0.3 MHz. The $K_L \to \pi^0\nu\bar{\nu}$ search using $\pi^0 \to e^+e^-\gamma$ used two large kaon beams ($0.1 \times 0.1$ m$^2$ at the CsI) with no beryllium absorber and a slightly higher proton beam intensity, resulting in a 12 MHz kaon flux. The photon veto signal loss with a 0.3 MHz kaon flux was about 20%; had we used the same photon veto cuts in the $\pi^0 \to e^+e^-\gamma$ method at high intensity, the signal loss would have been 96%! Fortunately, the charged vertex constraint was very effective at reducing the background, which allowed the photon veto cuts to be relaxed in order to increase the signal acceptance. Most of the potential 96% signal loss at 12 MHz flux is from the photon veto in the beam hole behind the CsI (see Fig. 1). The need to increase the kaon flux by yet another large factor makes this problem even more severe. A faster detector signal from either Cherenkov media (if there is enough light for low-energy photons) or from signal shaping will be necessary for a $K_L \to \pi^0\nu\bar{\nu}$ search to reach the SM sensitivity. Reducing the electronic noise will also help improve the signal efficiency of the photon veto system.

### 3.3 $K_L \to \pi^0 e^+e^-$

Using our full data set from the rare decay configuration (see end of Sec. 2) our single event sensitivity for the decay $K_L \to \pi^0 e^+e^-$ is $\sim 10^{-10}$, which is a factor of 10 to 100 away from reaching the SM sensitivity. The background from the decay $K_L \to e^+e^-\gamma\gamma$ is also at the $10^{-10}$ level, which means that $K_L \to \pi^0 e^+e^-$ will be dominated by background unless it is enhanced by nonstandard model effects. The background from $K_L \to \pi e\nu$ with a misidentified pion and two accidental photons is at the $10^{-12}$ level; this small background is due to the excellent pion rejection of both the CsI electromagnetic calorimeter and the TRD system.

## 4 Indirect CP Violation in $K_L \to \pi^+\pi^-e^+e^-$

The decay $K_L \to \pi^+\pi^-\gamma$ has both a CPC direct emission M1 amplitude and a CP-violating inner brem (IB) amplitude. The interference between these two amplitudes results in a CP-violating polarization that can be measured if the photon converts to an $e^+e^-$ pair. The decay $K_L \to \pi^+\pi^-e^+e^-$ internally converts the photon, and thus, provides another opportunity to observe indirect CPV.

Indirect CPV in $K_L \to \pi^+\pi^-e^+e^-$ is expected to cause an asymmetry in the angle between the $\pi^+\pi^-$ and $e^+e^-$ decay planes.[3] Defining this angle to be $\phi$, CP invariance requires that the number of events at $\phi$ is the same as the number of events at $-\phi$. The

asymmetry in the $\phi$ distribution is defined to be

$$A_\phi \equiv \frac{N(0 < \phi < \pi/2) - N(\pi/2 < \phi < \pi)}{N(0 < \phi < \pi/2) + N(\pi/2 < \phi < \pi)}, \quad (1)$$

where $N(\pi/2 < \phi < \pi) = N(-\pi/2 < \phi < 0)$ due to the symmetry $dN/d\phi(\phi) = dN/d\phi(\phi + \pi)$.

The predicted asymmetry and decay amplitudes are shown in Fig. 4 as a function of the $e^+e^-$ energy (i.e., the virtual photon energy) in the kaon center-of-mass frame. The IB amplitude dominates at small virtual photon energies, while the M1 amplitude dominates at higher virtual photon energies. The asymmetry results from the interference between these two amplitudes, and is maximal when the two amplitudes have approximately the same magnitude. The asymmetry integrated over all phase space is predicted to be 14% so the effect should be large. The predicted $\phi$ distribution[3] is

$$\frac{dN}{d\phi} = \Gamma_1 \cos^2(\phi) + \Gamma_2 \sin^2(\phi) + \Gamma_3 \sin(2\phi), \quad (2)$$

and is shown in Fig. 5 without the inner brem term because our experiment has very little sensitivity for IB events, which tend to have $e^+e^-$ tracks that are close together. The pure M1 term (dashed) in Fig. 5 is symmetric about $\pi/2$, and thus, has no net asymmetry. The interference term is clearly asymmetric about $\pi/2$, and thus, has a nonzero value of $A_\phi$. The sum of the two terms is shown by the thick solid curve, and qualitatively indicates the CP-violating signal that we are searching for experimentally.

Now that the expected CP-violating behavior for $K_L \to \pi^+\pi^-e^+e^-$ has been outlined, we can look for this effect in our data. For this search, we used the configuration for rare decays as explained at the end of Sec. 2.

The first step in the analysis is to cleanly identify the $K_L \to \pi^+\pi^-e^+e^-$ decay mode, which has previously not been observed. Based on a small sample of 36 events, a branching fraction of $[3.2 \pm 0.6(stat.) \pm 0.4(syst.)] \times 10^{-7}$ has already been reported by our collaboration.[4] A preliminary $\pi^+\pi^-e^+e^-$ invariant mass spectrum is shown in Fig. 6(a) for our full data set after all cuts, and contains 1766 $K_L \to \pi^+\pi^-e^+e^-$ events on a background of 45 events. The small background is due mainly to $K_L \to \pi^+\pi^-\pi^0_D$, where $\pi^0_D$ indicates the Dalitz decay $\pi^0 \to e^+e^-\gamma$.

The $\phi$ distribution without acceptance corrections is shown in Fig. 6(b) for the full data sample, and is compared with two Monte Carlo samples. The histogram is from a Monte Carlo using the SM matrix element that predicts an angular asymmetry. The dashed curve is from a Monte Carlo using the standard matrix element except that CPV

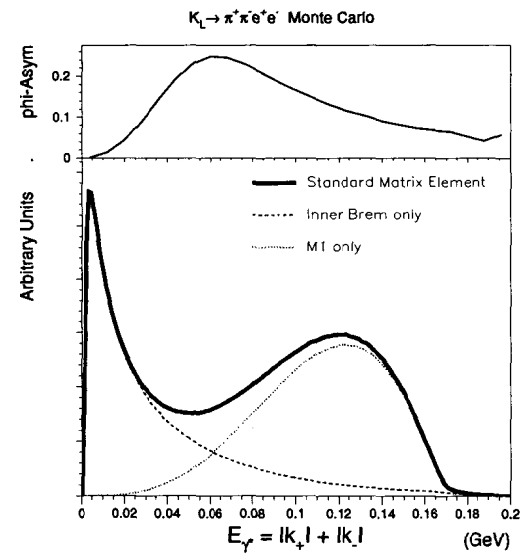


Fig. 4. The predicted angular asymmetry is shown as a function of the virtual photon energy in the kaon rest frame (top). The bottom plot shows the contributions to the matrix element from inner brem and direct emission amplitudes.

has been turned off by setting the relative phase between the M1 and IB amplitudes to be $90^0$. It is clear that our data favor the model with CPV. At the time of this conference a result was not available, but since then a preliminary result has been announced[5] and is $A_\phi = 13.5 \pm 2.5(stat.) \pm 3.0(syst.)\%$.

## 5 $K_L \to \pi^0\gamma\gamma$

The decay $K_L \to \pi^0\gamma\gamma$ is of interest because it can be used to estimate the CPC contribution to $K_L \to \pi^0 e^+e^-$. The CPC two-photon intermediate state $K_L \to \pi^0\gamma\gamma \to K_L \to \pi^0 e^+e^-$ is very small if only the S-wave $\gamma\gamma$ state is considered using $p^4$ calculations in Chiral Perturbation Theory (ChPT). This lead to the idea in the late 1980s that $K_L \to \pi^0 e^+e^-$ might be dominated by direct CPV if the SM is correct.[6,7] However, the first measurements of $B(K_L \to \pi^0\gamma\gamma)$ (Refs. 8 and 9) were about three times larger than the prediction for this mode, which cast doubt on the validity of the CPC predictions for $K_L \to \pi^0 e^+e^-$.

Shortly after the first measurements of $B(K_L \to \pi^0\gamma\gamma)$, ChPT calculations including $p^6$ corrections and vector meson exchange predicted a branching fraction consistent with experiment. However, these new calculations also predicted a much larger CPC contribution to $K_L \to \pi^0 e^+e^-$, such that the CPC and CPV contributions were comparable. The increase in the CPC amplitude arises from the spin 2 (D-wave) component of the vector meson and $p^6$ corrections, and it is not helicity suppressed as was for the case of the $p^4$ (spin 0) predictions. Another new prediction is the presence of a low-side tail in the $m_{\gamma\gamma}$ distribution, where the $\gamma\gamma$ subscript refers to the two photons not associated with the $\pi^0$. The previous experiments did not have enough sensitivity to see this tail. Our new measurement in KTeV has sufficient statistics to observe the low-side $m_{\gamma\gamma}$ tail and to compare with ChPT. The data presented here were collected simultaneously with the $K_{L,S} \to \pi^0\pi^0$ events used in the measurement of $\mathrm{Re}(\epsilon'/\epsilon)$.

The detection of $K_L \to \pi^0\gamma\gamma$ is difficult because there are not enough kinematic constraints to make a traditional invariant mass plot that clearly identifies the signal. We therefore rely heavily on a Monte Carlo simulation to predict the background levels. The background from $K_{L,S} \to \pi^0\pi^0$ is removed by discarding events that have an $m_{\gamma\gamma}$ value within a 0.06 GeV window around the $\pi^0$ mass. The dominant background is from $K_L \to 3\pi^0$, in which two photons "fuse" with other photons and appear as a four-photon event. The strategy for reducing this background is to use the transverse cluster shapes at the CsI calorimeter. Using simulated photon showers as a template,

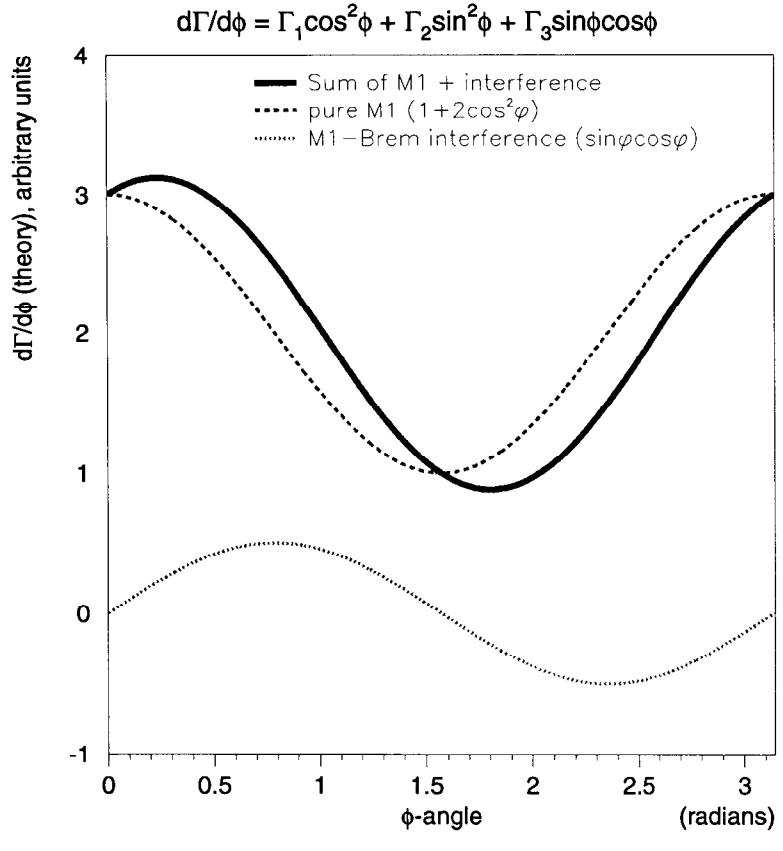


Fig. 5. The predicted $\phi$ distribution is shown for M1 direct emission (dashed), M1-brem interference (dots), and the sum of M1 and interference (solid).

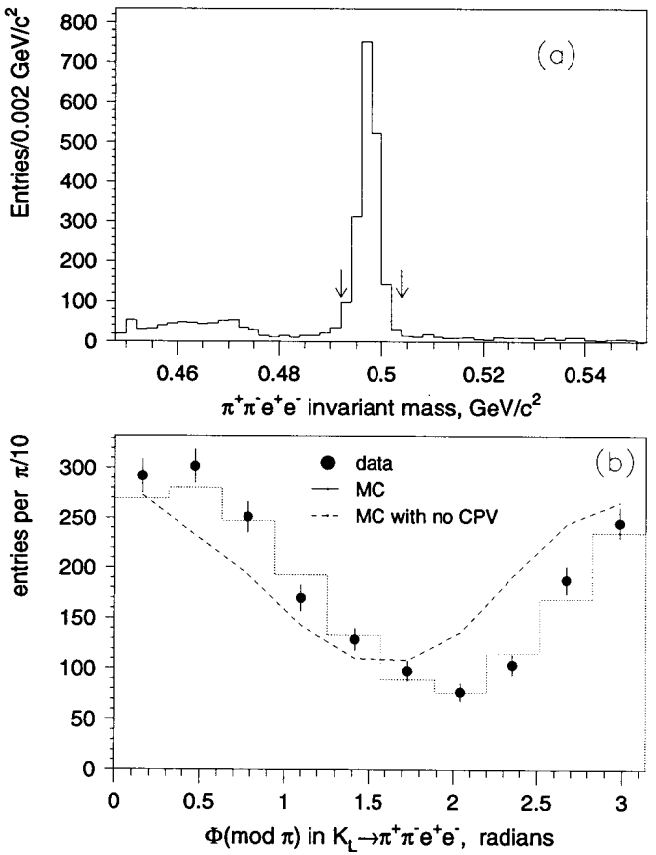


Fig. 6. Our preliminary $\pi^+\pi^-e^+e^-$ invariant mass spectrum is shown in (a) after all the analysis cuts. The arrows show the mass window (0.492 to 0.504 GeV/c$^2$) used to select $K_L \to \pi^+\pi^-e^+e^-$ events for the angular distribution shown in (b). Events at $\phi$ and $\phi + \pi$ are plotted in the same bin. The dots are for data, the histogram is the Monte Carlo using the SM matrix element, and the dashed curve is a Monte Carlo with no CPV in the matrix element.

we have computed a "shape" $\chi^2$ for each cluster using the central $3 \times 3$ crystal energies. The maximum shape $\chi^2$ of the four clusters is shown in Fig. 7 for each $K_L \to \pi^0\gamma\gamma$ candidate. A peak is clearly seen at small values of the shape $\chi^2$, and we interpret this peak as the $K_L \to \pi^0\gamma\gamma$ signal. The histogram in Fig. 7 shows the Monte Carlo prediction of the $K_L \to 3\pi^0$ background, which is absolutely normalized to the number of $K_L \to 2\pi^0$ decays. After applying a cut of shape $\chi^2 < 2.0$, a preliminary $m_{\gamma\gamma}$ spectrum is shown in Fig. 8. There are 796 signal events on a background of $111 \pm 14$. This is a factor of 12 larger than the statistics used in the previous best measurement. Normalizing this sample to $K_L \to 2\pi^0$ gives a preliminary branching fraction of

$$B(K_L \to \pi^0\gamma\gamma) = 1.76 \pm 0.06(stat.) \pm 0.09(syst.) \times 10^{-6}, \quad (3)$$

where about half of the systematic uncertainty is related to the determination of the $K_L \to 3\pi^0$ background, and the remaining uncertainty is from the $K_L \to 2\pi^0$ branching ratio (2.1%) and the offline analysis cuts (3.3%).

The number of events with $m_{\gamma\gamma} < 0.240$ GeV/c$^2$ is $83 \pm 14 \pm 9$, and it is the first observation of the low-mass events for this decay mode. This corresponds to about 14% of the total decay rate after correcting for the unobserved events near the $\pi^0$ mass. The shape $\chi^2$ distribution for these low-mass events is shown in the the inset of Fig. 7, and clearly shows a signal peak. The next step is to use the data to extract the vector meson coupling, $a_V = -0.8 \pm 0.1$. This coupling is then used to calculate the CPC part of $K_L \to \pi^0e^+e^-$ and results in

$$B_{CPC}(K_L \to \pi^0e^+e^-) = 1 - 2 \times 10^{-12}, \quad (4)$$

which is a few times smaller than the expected rate from direct CPV.

There is also an indirect CPV contribution from the small CP-even part of the $K_L$, which can be determined from a measurement of $B(K_S \to \pi^0e^+e^-)$. The current 90% upper limit is $B(K_S \to \pi^0e^+e^-) < 1.1 \times 10^{-6}$ from NA31 at CERN.[10] During the collection of $K^0 \to \pi\pi$ events for the Re($\epsilon'/\epsilon$) measurement we saved events from the regenerator beam that had the topology of a $K_S \to \pi^0e^+e^-$ decay. Preliminary analysis indicates that we have a sensitivity of $\sim 10^{-7}$; if there is no background, this translates into a sensitivity of a *few* $\times 10^{-10}$ on the indirect CPV contribution to $K_L \to \pi^0e^+e^-$.

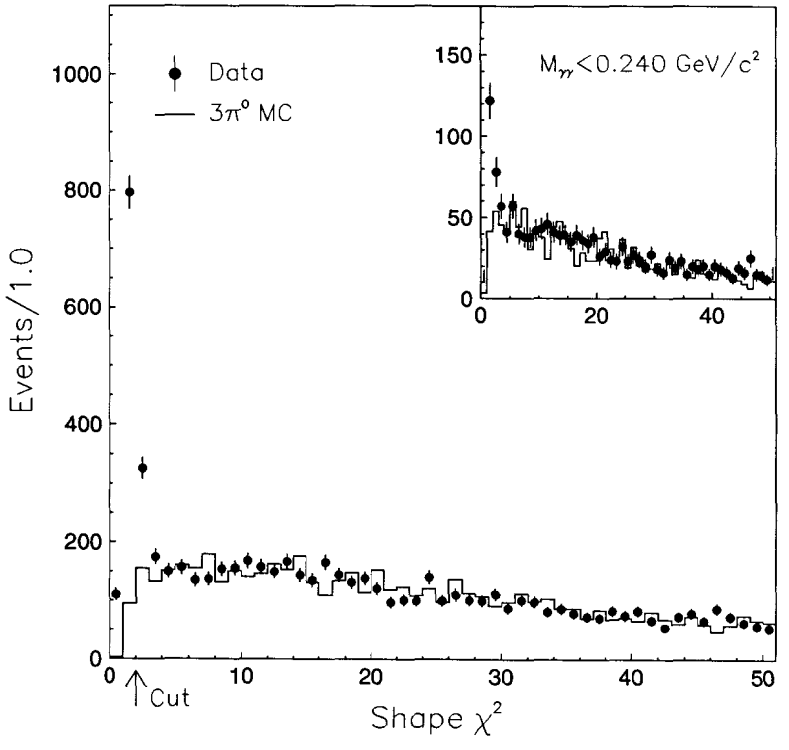


Fig. 7. The maximum transverse shape $\chi^2$ of the four photons for each $K_L \to \pi^0\gamma\gamma$ candidate after all offline software cuts except the $\chi^2$ cut (*preliminary*). The inset shows the same distribution for events with $m_{\gamma\gamma} < 0.240$ GeV/$c^2$. The data are shown by dots; the histogram is from a Monte Carlo simulation of $K_L \to 3\pi^0$ events.

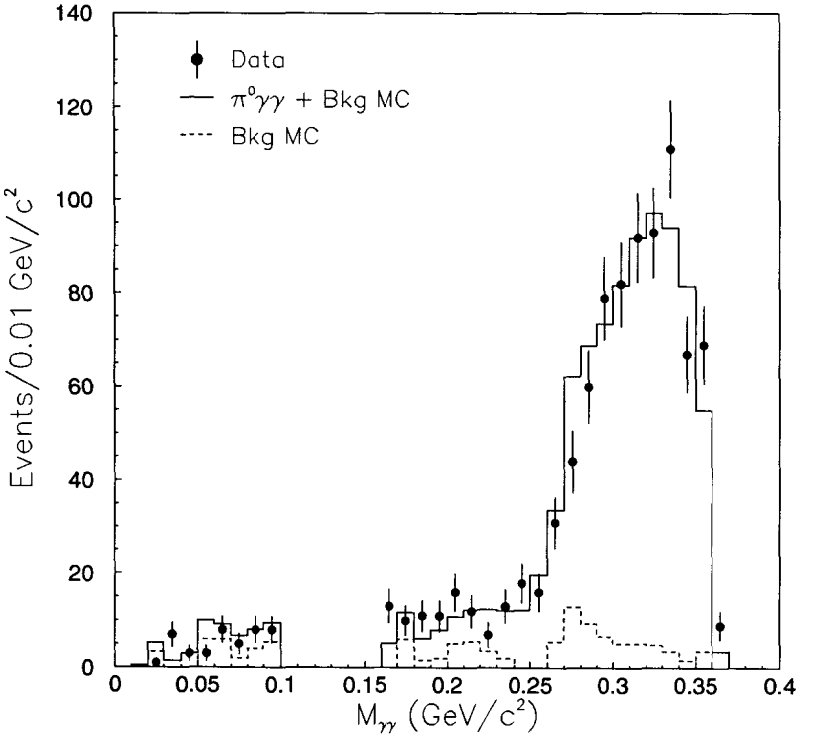


Fig. 8. *Preliminary* $m_{\gamma\gamma}$ mass spectrum for $K_L \to \pi^0\gamma\gamma$ candidates. These two photons are not associated with the $\pi^0$.

# 6 Conclusions

To summarize, the impact and status of KTeV on CP-violating phenomenon in the kaon system is shown in Table 2. A gauge of progress is shown in the column labeled "additional sensitivity needed to reach the SM."

| Physics | | *Preliminary* KTeV result | Additional sensitivity to reach SM |
|---|---|---|---|
| $\mathrm{Re}(\epsilon'/\epsilon)$ | $D_{CPV}$ | not yet | $< 10$ ? |
| $K_L \to \pi^0\nu\bar{\nu}$ with $\pi^0 \to \gamma\gamma$ | $D_{CPV}$ | $< 1.6 \times 10^{-6}$ | $10^5$ |
| $K_L \to \pi^0\nu\bar{\nu}$ with $\pi^0 \to e^+e^-\gamma$ | $D_{CPV}$ | $< 5.9 \times 10^{-7}$ | $10^5$ |
| $K_L \to \pi^0 e^+e^-$ | $D_{CPV} + I_{CPV}$ | not yet | $10^2$ |
| $K_L \to \pi^0\gamma\gamma \to \pi^0 e^+e^-$ | CPC | $1 - 2 \times 10^{-12}$ | — |
| CP-violating asymmetry in $K_L \to \pi^+\pi^-e^+e^-$ | $I_{CPV}$ | "evidence" | none |

Table 2. Summary of CPV searches in the KTeV experiment. $D_{CPV}$ and $I_{CPV}$ refer to Direct and Indirect CPV.

For the $\mathrm{Re}(\epsilon'/\epsilon)$ measurement, we expect to soon release a result based on 25% of our data. The statistical precision will be $3 \times 10^{-4}$. The systematic uncertainty will depend on our ability to understand the beam region of the drift chambers, and on the CsI calibration for photons with energies below 4 GeV.

On the $K_L \to \pi^0\nu\bar{\nu}$ "golden" mode, we are a dismal five orders of magnitude away from reaching the SM sensitivity using the $\pi^0 \to \gamma\gamma$ technique, and seven orders of magnitude away from the ultimate goal of observing $\sim 100$ events in order to measure the CKM parameter $\eta$ with several percent accuracy. Two orders of magnitude in sensitivity can be gained by running for 100 days instead of just one day, and another order of magnitude can be gained using currently available proton intensities. How to obtain the remaining four orders of magnitude is still not clear. The physics potential in this mode is fantastic but it is not evident that current technology will work. New ideas will most likely be a necessary ingredient for observing this mode at the SM level.

Although our sensitivity to $K_L \to \pi^0 e^+e^-$ is still a factor of 100 away from the SM, we have made progress on determining its CPC contribution. Our measurement of the $K_L \to \pi^0\gamma\gamma$ branching fraction and of its $m_{\gamma\gamma}$ spectrum can be combined with ChPT calculations to predict the CPC contribution to $K_L \to \pi^0 e^+e^-$. We find that $B_{CPC}(K_L \to \pi^0 e^+e^-) = 1 - 2 \times 10^{-12}$.

Finally, we have shown new evidence of indirect CPV in the angular distribution of the $K_L \to \pi^+\pi^-e^+e^-$ decay planes.[5] This is the fourth and largest observed manifestation of CPV since the initial discovery of $K_L \to \pi^+\pi^-$.

# References


[1] T. Nakaya, presented at the *Flavor Changing Neutral Current Conference*, Santa Monica, CA, 1997; KTeV Collaboration, hep-ex/9806007 (1998).

[2] K. Hanagaki, "Search for the Decay $K_L \to \pi^0\nu\bar{\nu}$," Ph. D. thesis, Osaka University, 1998.

[3] L. M. Sehgal and M. Wanninger, "CP Violation in the Decay $K_L \to \pi^+\pi^-e^+e^-$," Phys. Rev. D **46**, 1035 (1992).

[4] J. Adams *et al.*, "Measurement of the Branching Fraction of the Decay $K_L \to \pi^+\pi^-e^+e^-$," Phys. Rev. Lett. **80**, 4123 (1998).

[5] A quantitative result on the $K_L \to \pi^+\pi^-e^+e^-$ angular asymmetry has recently been announced by our collaboration at the *HQ98 Conference* at Fermilab (October 1998).

[6] G. Ecker, A. Pich, and E. De Rafael, Phys. Lett. **189**, 363 (1987).

[7] G. Ecker, A. Pich, and E. De Rafael, Nucl. Phys. B **303**, 665 (1988).

[8] G. Barr *et al.*, Phys. Lett. B **284**, 440 (1992).

[9] V. Papadimitriou *et al.*, Phys. Rev. D **44**, 573 (1991).

[10] G. Barr *et al.*, Phys. Lett. B **304**, 381 (1993).